

# Phase Behaviors and Dynamics of Active Particle Systems In Double-Well Potential

Lu Chen\*,<sup>1</sup> Baopi Liu,<sup>2</sup> and Ning Liu<sup>†3</sup>

<sup>1</sup>*School of Physics, Changchun Normal University, Changchun, Jilin 130032, China*

<sup>2</sup>*Complex Systems Division, Beijing Computational Science Research Center, Beijing 100193, China*

<sup>3</sup>*School of Mathematics and Physics, Anqing Normal University, Anqing, Anhui 246133, China*

(\*Electronic mail: ningliu@mail.bnu.edu.cn)

(Dated: 4 September 2024)

In this paper, we investigate the phase behaviors and dynamics of self-propelled particles with active reorientation in double-well potential. We observe the self-propelled particles exhibit flocking and clustering in an asymmetric potential trap. By MD simulations, we obtain a phase diagram of flocking with active reorientation and potential asymmetry as parameters. We compare the responses of inactive and active particles to the potential. It shows that active reorientation of particles amplifies the degree of aggregation on one side in the asymmetric potential well. Furthermore, we calculate the mean squared displacement and identify distinct diffusion regimes. These results highlight active particles with active reorientation exhibit greater sensitivity in double-well potentials.

## I. INTRODUCTION

The self-propulsion of active particles is very common in microorganisms. Systems composed of such particles with sustained self-propulsion capabilities exhibit a wealth of phenomena, such as phase separation<sup>1-3</sup>, flocking<sup>4-7</sup> and synchronization<sup>8,9</sup>. In all these systems, interactions occur only between particles without any external forces. However, if active particles are exposed to an external field, it will inevitably affect their trajectories and collective dynamics.

There has been some research on the motion of active particles in an external field<sup>10-13</sup>. Potentials can be used to create reconfigurable materials, such as guiding colloidal particle assembly<sup>14,15</sup>. Furthermore, recent studies on the collective dynamics of active Brownian particles have revealed the impact of gravity<sup>16</sup>, external magnetic fields<sup>17,18</sup> and harmonic potential fields<sup>11,19,20</sup>. Among various types of potentials, the double-well potential plays a significant role in several physical systems. In the work of Marchenko et al., they reveal that the underdamped motion of particles in space-periodic potentials is equivalent to overdamped motion within velocity space, resembling an effective double-well potential<sup>21</sup>. In the work of Militaru et al., they study the effect of non-conservative forces on the escape dynamics of active particles in non-equilibrium systems by using a bistable optical potential trap to capture silica nanoparticles, finding an optimal correlation time that maximizes the escape rate<sup>23</sup>. Caprini et al. investigate the escape behavior of active particles in a double-well potential, revealing an optimal persistence time that minimizes the escape time and showing that repulsive interactions between active particles lead to correlated escape, a mechanism absent in systems without active particles<sup>24</sup>. The double-well potential models these transitions, representing distinct functional states based on external signal strength or duration<sup>25</sup>.

In our previous work<sup>26</sup>, we proposed a new active model consisting of self-propelled particles with active reorientation (AR). In this model, in addition to translational motion, the

particles can also adjust their orientation through active reorientation. This concept of active reorientation is inspired by animal groups in nature<sup>27,28</sup>, which actively adjust their orientation to avoid collisions when encountering obstacles. In this paper, we focus on the phase behaviors and dynamics of self-propelled particles with AR in a double-well potential, exploring the competition between AR and the external potential. First, we introduce the active system and the choice of potential. We then explore the relationship between phase behaviors (such as flocking and clustering) in this system and the parameter of asymmetry. Next, we study the dynamics of the system by examining the time dependence of particle number flow in symmetric and asymmetric wells, and by comparing the effects of the double-well potential in systems with and without active reorientation. Finally, we analyze the mean squared displacements (MSDs) to identify different diffusion regimes. The last section presents our conclusions.

## II. DYNAMIC MODEL

Here we consider an active model that is based on a previous work<sup>26,29</sup>. The model consists of  $N$  self-propelled disks in the two-dimensional box of length  $L_x$  in the  $x$  direction and  $L_y$  in the  $y$  direction. Self-propelled disks with a diameter  $d$ , which are modeled as active Brownian particles. The location of particle  $i$  is represented by the vector  $\mathbf{r}_i$ , and the direction of its velocity is expressed by the orientation  $\theta_i$  of the polar axis  $\mathbf{p}_i \equiv (\cos \theta_i, \sin \theta_i)$ . The dynamics of particle  $i$  is governed by the following overdamped Langevin equations:

$$\dot{\mathbf{r}}_i = v_0 \mathbf{p}_i \prod_{j=1, j \neq i}^N \varepsilon(r_{ij} - 2R) + \mu \mathbf{F}_i^{\text{in}} + \gamma \mathbf{F}_i^{\text{ex}} + \sqrt{2D_T} \zeta_i(t) \quad (1)$$

$$\dot{\theta} = \sum_{j=1, j \neq i}^N \alpha \delta(t) \varepsilon(2R - r_{ij}) \frac{\mathbf{r}_{ij} \times \mathbf{p}_i}{|\mathbf{r}_{ij} \times \mathbf{p}_i|} \cdot \hat{\mathbf{z}} + \sqrt{2D_R} \xi_i(t). \quad (2)$$

The first equation describes the translational motion of disk  $i$ . The magnitude of self-propelled velocity is denoted by  $v_0$ .  $\mathbf{r}_{ij} \equiv \mathbf{r}_i - \mathbf{r}_j$ , the distance between the center of particles is  $r_{ij} \equiv |\mathbf{r}_i - \mathbf{r}_j|$ . Unit direction vector between particle  $j$  to  $i$  is  $\hat{\mathbf{r}}_{ij} = \frac{\mathbf{r}_{ij}}{r_{ij}}$ .  $\varepsilon(x)$  is the Heaviside step function. If  $r_{ij} < d$ , then  $\varepsilon = 1$ , otherwise  $\varepsilon = 0$ .  $\mu$  is the mobility.  $\mathbf{F}_i^{\text{in}}$  is the force exerted on particle  $i$  by other active particles, expressed as  $\mathbf{F}_i^{\text{in}} = \sum_{j=1, j \neq i}^N \mathbf{F}_{ij}$ . Here,  $\mathbf{F}_{ij}$  is the force acting on disk  $i$  from particle  $j$ ,  $\mathbf{F}_{ij} = k(d - r_{ij})\hat{\mathbf{r}}_{ij}$ , if  $r_{ij} < d$ ; else  $\mathbf{F}_{ij} = 0$ . Parameter  $k$  represents the strength of two-body interaction between particles.  $\mathbf{F}_i^{\text{ex}} = -\nabla U$ , arises from an asymmetric potential  $U$ .  $\gamma$  is the friction.

The second equation describes the rotational motion of particle  $i$ . The first item describes the effect of active reorientation on particle  $i$ .  $\alpha\delta(t)$  is the angular velocity, which is generated as a result of active reorientation acting on the colliding particles.  $\hat{\mathbf{z}}$  is a normal vector of the plane pointing to the reader.  $\alpha$  is a positive value to mitigate the collision between two disks in a collision.  $\zeta_i(t)$  and  $\xi_i(t)$  are Gaussian white noises with zero mean, that is  $\langle \zeta_i(t) \rangle = 0$ ,  $\langle \xi_i(t) \rangle = 0$  and  $\langle \zeta_i(t)\zeta_j(t') \rangle = 2D_t\delta_{ij}\delta(t-t')$ ,  $\langle \xi_i(t)\xi_j(t') \rangle = 2D_r\delta_{ij}\delta(t-t')$ .  $D_t$  and  $D_r$  are translational and rotational diffusion coefficients, respectively. Then we introduce the characteristic length scale  $d$  and the time scale  $\mu k$ . So other parameters in this paper are scaled as:  $\hat{\mathbf{r}}_i = \frac{\mathbf{r}_i}{d}$ ,  $\hat{\mathbf{t}} = \mu k t$ ,  $\hat{L}_x = \frac{L_x}{d}$ ,  $\hat{L}_y = \frac{L_y}{d}$ ,  $\hat{v}_0 = \frac{v_0}{\mu k d}$ ,  $\hat{D}_t = \frac{D_t}{\mu k}$  and  $\hat{D}_r = \frac{D_r}{\mu k}$ . In the following discussions, we use dimensionless variables. Additionally, we will omit the hats when referring to any quantities mentioned in the above equations.

Herein we consider  $U$  as a quasi-one-dimensional potential, where  $U(x, y)$  expressed as follows:

$$U(x, y) = a(z^4 - z^2) + cz + b\bar{z}^2 \quad (3)$$

Here  $z = k(x + y)$  and  $\bar{z} = k(x - y)^{20}$ . The potential can be defined with an asymmetric parameter  $c$  and its strength is denoted as  $a$ .  $U(x, y)$  is illustrated in Fig. 1. In our simulation

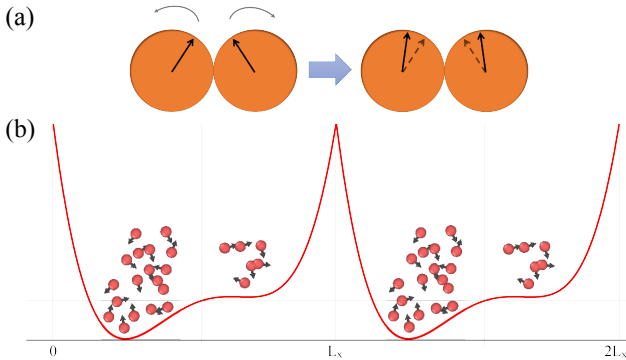


FIG. 1. Active particles in double-well potential. The orange circles schematically show the state of particles before and after overlapping due to active reorientation. The red curve below presents the projection of the asymmetric potential  $U(x, y)$  in the  $x$ -direction.

in this paper, the parameters of  $U$  are sets  $1/30$ ,  $a$  is 1, and  $b$

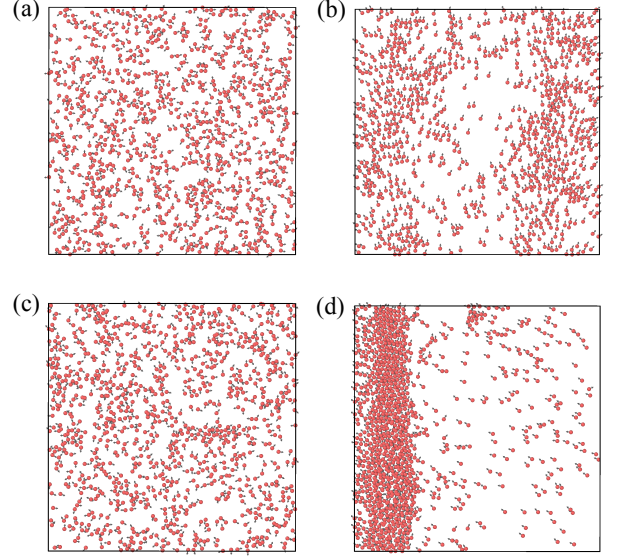


FIG. 2. Snapshots of the active system in the initial state and steady state. (a) initial state (disordered phase) with  $c = 0$ . (b) steady state (flocking) with  $c = 0$ . (c) initial state (disordered phase) with  $c = -0.5$ . (d) steady state (flocking and clustering) with  $c = -0.5$ . The arrow represents the direction of the polarity. The other parameters are  $N = 1000$ ,  $D_t = 0.005$ ,  $D_r = 0.005$ ,  $\alpha = 0.02$  for all figures.

is  $1/1.5$ . And we process the potential under periodic conditions. The total integration time was set to exceed  $10^6$ , while the integration step time is  $10^{-2}$ . We fix self-propulsion velocity  $v_0 = 0.1$ . We numerically solve Eqs. (1) and (2) using periodic boundary conditions with a square box of length  $L$ . The relevance of crowding is controlled by the packing fraction  $\phi = \frac{N\pi(d/2)^2}{L^2}$ . We have performed molecular dynamics simulations with  $N = 1000$  to 16,000 particles to check the finite size effect. The number of particles has no obvious effect on the result, the difference is only reflected in the fluctuation of the physical quantity. The following result is  $n = 10^3$  particles in  $5 \times 10^6$  steps with  $D_t = 5 \times 10^{-3}$ ,  $D_r = 5 \times 10^{-3}$  and  $\phi = 0.2$ . Equations are iteratively updated for each particle, and a single simulation step is counted after all the particles have been updated once. We initiate the simulation with a random homogeneous distribution of particles in the box with random orientations. By simulation, in Fig. 2, we present snapshots of initial states and steady states in symmetric ( $c = 0$ ) and asymmetric ( $c = -0.5$ ) potential wells. We find that when particles are in symmetric potential from the initial state [ Fig. 2(a)], the steady state of the system exhibits a state of flocking as shown in Fig. 2(b). The position distribution of the system particles is uniform in the  $X$  direction. However, in asymmetric potential, the system also starts with the homogeneous state [ Fig. 2(c)], and eventually evolves into a state in which particles will aggregate in the deeper side of the potential well as shown in Fig. 2(d). In the meantime, there is a state of flocking and clustering at the same time. So compared to the situation where there is no altitude gradient in the poten-

tial field ( $c = 0$ ), it seems that the asymmetry of the potential field causes the uneven distribution of particles in space.

### III. PHASE BEHAVIORS

We find that flocking and clustering appeared in the stability of system evolution, which did not appear in the previous studies. So based on the findings above, to quantify these effects and characterize the behaviors of phases in the system, we introduce order parameters. For flocking, we measure the net velocity, which is expressed as  $M = \sqrt{\langle \cos \theta \rangle^2 + \langle \sin \theta \rangle^2}$ , where the average  $\langle \rangle$  is taken over all  $N$  particles. When  $M$  approaches 0, it implies that the system is in a disordered state, and when  $M$  approaches 1, it indicates that the system is in a highly ordered state. To quantitatively identify the clustering phase of the system that separates into dense clustered and dilute gas-like states, we measure the local area density of each particle<sup>30</sup>. The local area density of each particle is the ratio of the area of each particle to the area of the polygon via a Voronoi tessellation of each particle. By numerical simulation, in this work, we set the threshold of local area density as 0.6. We introduce the order parameter  $\rho_c$  to describe clustering, which is the sum of the fraction of particles with its local area density larger than 0.6. Its math expression is shown as:  $\rho_c = \sum P(\phi_i > 0.6)$ .

We execute with 100 initial positions in the simulation to get average results. Fig. 3(a) shows the simulation results for the dependence of  $M$  on  $t$  under different values of  $c$ . We observe that with the increase of  $|c|$ ,  $M$  in the steady state would gradually decrease. Subsequently, we test the evolution of  $\rho_c$  over time under the same condition above as shown in Fig. 3(b). When  $|c|$  is relatively small, the system initially exhibits the aggregation of particles, gradually accumulates saturation to a larger scale cluster, and then gradually dissipates. However, when  $|c|$  is large enough, the particles in the system gradually gather into a large cluster and no longer dissipate. By combining these two figures, it can be found that there is obvious flocking in the steady state without aggregation in the symmetric potential well ( $c = 0$ ). And when  $|c|$  is large, the steady state of the system exhibits both clustering and flocking state. This is consistent with what is shown in Fig. 2. These results demonstrate a negative correlation between  $M$  in the steady state and  $|c|$  and a positive correlation between  $\rho_c$  in the steady state and  $|c|$ .

Next, we explore the steady state of the system, focusing mainly on flocking. We first test the relationship between flocking ( $M$ ) and the parameter of asymmetry  $c$  under different  $\alpha$  values, as shown in Fig. 4(a). We find that when  $\alpha$  is small (e.g.,  $\alpha = 0.02$ ), two behaviors exist: when  $c$  is small ( $c < 0.5$ ), flocking ( $M$ ) is essentially independent of  $c$ . However, when  $c$  increases ( $c > 0.5$ ),  $M$  decreases with the increase of  $c$ . When  $\alpha$  increases (e.g.,  $\alpha = 0.08, 0.15$ ), the former behavior (when  $c$  is small) is consistent with the above situation, but in the latter behavior (when  $c$  is large),  $M$  also becomes independent of  $c$ , showing a global insensitivity to  $c$ . When  $\alpha$  continues to increase (e.g.,  $\alpha = 0.4$ ),  $M$  shows a significant decreasing trend with the increase of  $c$ . Finally,

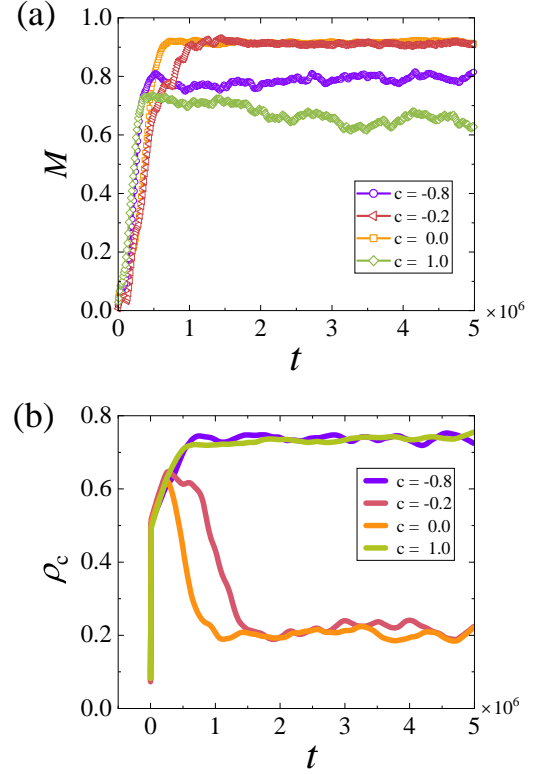


FIG. 3. (a)  $M$  and (b)  $\rho_c$  as a function of  $t$  under different values of  $c$ . Simulation parameters:  $\alpha = 0.02$ .

as  $\alpha$  increases to a certain extent (e.g.,  $\alpha = 0.6, 0.8$ ), the entire system exhibits a completely disordered state and is also independent of  $c$ .

These findings suggest a competitive relationship between activity and asymmetry in this system. To further explore the competitive relationship between the two, we test the contour map of flocking about  $c$  and  $\alpha$ , where the color represents the order parameter of flocking  $M$  in Fig. 4(b). It is evident that when  $\alpha$  is small, the larger the asymmetry  $c$  of the potential, the smaller the  $M$ . When  $\alpha$  is large, activity becomes the dominant factor.  $\alpha = 0.4$  can be considered a critical  $\alpha$ , serving as the boundary between ordered and disordered states of the system. It is also clear that changes in activity have a more significant impact on  $M$  compared to the degree of asymmetry.

### IV. DYNAMICS

The dynamics of the system are studied by analyzing the fraction of particles in the left and right wells in the simulation domain. Here we use  $n_1$  and  $n_2$  to represent the number of particles in left and right well, respectively. Fig. 5 presents the dependence of  $n_1$  and  $n_2$  on time series in the symmetric and asymmetric potentials. In Fig. 5(a), when  $c$  is 0, we find that the number of particles distributed in the left and right  $x$ -axis at the first stage of evolution shows a state of periodic ex-

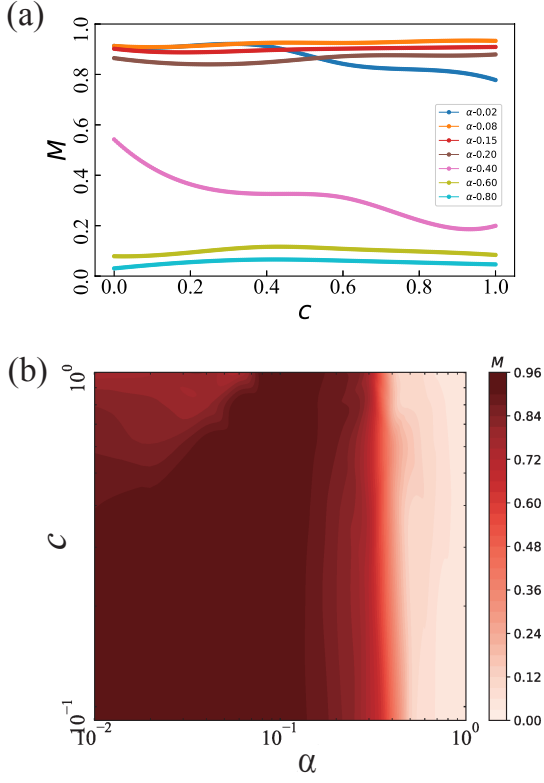


FIG. 4. (a) Flocking order parameter  $M$  versus  $c$  for different values of  $\alpha$  as denoted in the key. (b) Simulations reveal dependence on both active reorientation  $\alpha$  and asymmetry parameter  $c$ . All data was averaged over time in a steady state.

change between the left and right positions over time, and then particles gradually distribute on both sides equally tending to be stable. The number of particles in the potential on the left and right of the x-axis is the same dynamically in the symmetric potential wells, which suggests the system does not exhibit directed motion in the x-axis in a symmetric potential. This is different from the situation where  $|c|$  is larger. As we can see from Fig. 5(b), when the parameter of asymmetry of the potential is -0.8, we find that particles in this potential gradually evolve from the uniform state in the position space to a phase separation state. It is shown that the particles are confined by the potential field in the lower region of the potential well. On the other side, there are essentially few particles. At the same time, We observe that when  $c$  is 0.2 as shown in Fig. 5(c), there seems to be a situation where the left and right sides exchange with each other just like the results with  $c$  is 0, but the exchange frequency is not as obvious as Fig. 5(a). Compared with Fig. 5(b), Fig. 5(d) shows that the degree of particle exchange at the left and right potential gradually decreases with the increase of  $|c|$ . These results indicate that the parameter of asymmetry in the potential field plays a crucial role in determining the capture of particles. Next, as a comparison, we explore the dynamics of an active system without active reorientation in the double-well potential which is shown in Fig. 6. First of all, we notice that the distribution of

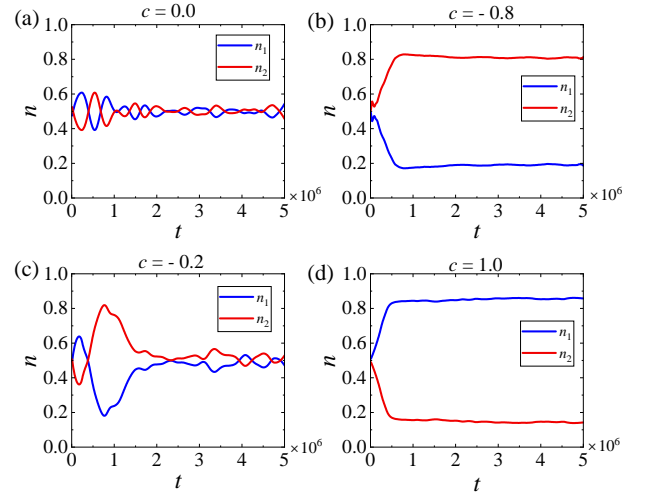


FIG. 5.  $n_1$  and  $n_2$  as a function of time for various values of  $c$  in this active system with active reorientation ( $\alpha = 0.02$ ,  $D_t = 0.005$ ,  $D_r = 0.005$ ).

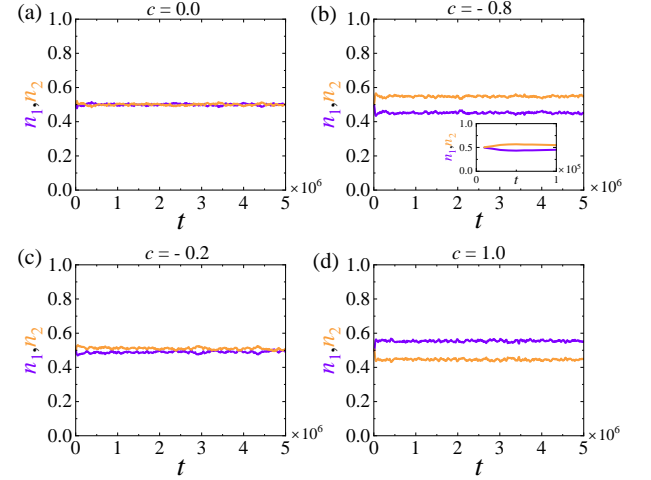


FIG. 6.  $n_1$  and  $n_2$  as a function of time for various values of  $c$  in this active system without active reorientation ( $\alpha = 0$ ,  $D_t = 0.005$ ,  $D_r = 0.005$ ).

particles in the left and right sides of the potential is uniform with  $c = 0$  [Fig. 6(a)] just like the results above [Fig. 5(a)]. As the value of  $|c|$  increases, particles also exhibit directed flow towards the deeper side of the potential field. Notably, the gap between  $n_1$  and  $n_2$  is smaller than the gap in the active system with active reorientation. This also indicates that active reorientation enhances the directed motion of the system in the asymmetric potential. In other words, active reorientation endows the system with a stronger ability for directed leadership compared to a system lacking active reorientation.

Then we average  $n_1$  in the Fig. 5 and Fig. 6 of time after 3,000,000 and obtain  $n_{1s}$  as the number of particles in the left potential in the steady state and standard deviation of  $n_{1s}$ . Fig. 7 presents  $n_{1s}$  as a function of different values of  $c$ . We observe that  $n_{1s}$  exhibits an anti-symmetric form con-

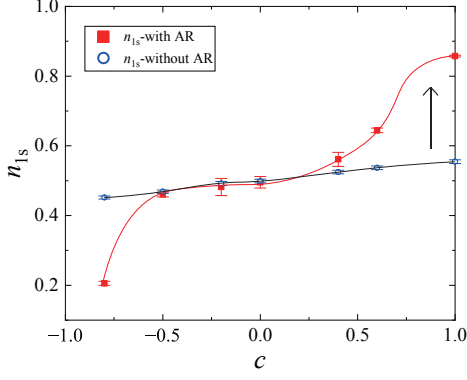


FIG. 7. A plot on the parameter of asymmetry  $c$  dependence of  $n_{1s}$  evaluated at steady state.

cerning  $c = 0$ . Diamond points shown in Fig. 7 demonstrate that when the value of  $|c|$  is less than 0.5, the steady state of the system demonstrates relatively uniform on both sides. When  $|c|$  is greater than 0.5, the steady-state exhibits an obviously asymmetric state with particles concentrating in the deeper side region. As for particles without active reorientation (circle points), the behavior of  $n_{1s}$  with  $c$  is consistent with that of the active reorientation case, but the degree of change is much smaller. It demonstrates that the amplification of active reorientation enhances the effect of asymmetry on the distribution of particles along the x-axis.

## V. DIFFERENT DIFFUSION REGIMES

In the active system of self-propelled particles moving in a double well potential, the dynamics can be influenced by both the underlying potential and the self-propulsion as well as the active rotation of the particles. So next we focus on the long time dynamic behaviors when the asymmetry parameter of potential increases by calculating the mean-squared displacement (MSD), which is

$$\langle r^2(t) \rangle = \frac{1}{N} \sum_{i=1}^N \langle [r_i(t) - r_i(0)]^2 \rangle \quad (4)$$

where  $r_i$  is the position of particle  $i$ , and  $N$  is the total number of particles in the studied system. As we know, the relationship between the MSDs and time  $t$  can be given by  $\langle r^2 \rangle \propto t^\nu$ . So we test MSD and get  $\nu$  in the x and y directions under different values of  $c$  both in the system with AR (Fig. 8(a) and (c)) and without AR (Fig. 8(b) and (d)). Fig. 8 shows that there is a clear difference in scaling behavior between particles with active reorientation and without active reorientation of MSD. First, we focus on the MSD of the system with AR in Fig. 8(a). We found that similar to the passive system, a brief period of diffusive motion is observed initially, followed by a transition to a subdiffusive regime due to the caging effect. While the subdiffusive phase consistently emerges, the subsequent superdiffusive behavior—known in the context of

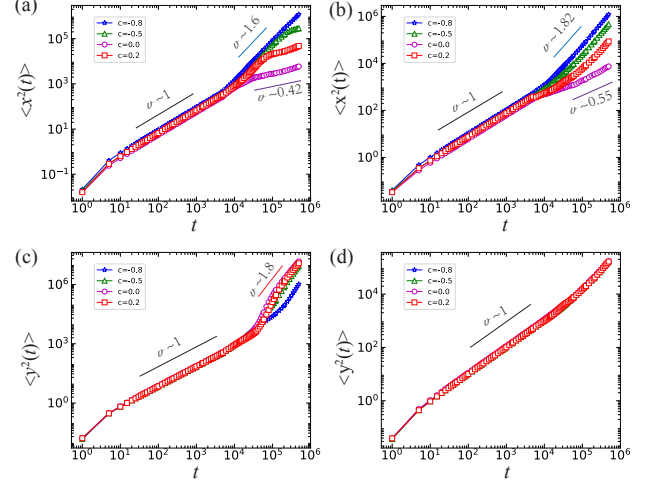


FIG. 8. The MSDs along the x and y directions versus time for various values of  $c = -0.8, -0.5, 0.0, 0.2$ . (a) MSDs in the x-direction of the system with and (b) without active reorientation. (c) MSDs in the y-direction of the system with and (d) without active reorientation. The solid lines represent the exponential fittings.

free active particles—is not universally observed. Its occurrence depends on the interplay between structural relaxation and the simultaneous decorrelation of rotational degrees of freedom<sup>31,32</sup>. Next comparing MSDs of AR and no AR systems, in the short time scale, both AR and no AR systems exhibit Brownian motion under different degrees of asymmetry. However, in the long time scale, it is found that in the x direction (Fig. 8(a) and (b)), the caging effect of the system with AR is significantly stronger (as indicated by a lower subdiffusion exponent) than that of the system without AR under the same asymmetry. This behavior is consistent with some previous findings. In the previous work<sup>33</sup>, researchers claim that the exponents  $\nu$  of the free particle consistently reveal the occurrence of caging in the form of pronounced minima and the enhancement of superdiffusion with increasing persistence length. Further, they confirm that superdiffusive behavior can be suppressed in the entire time window which is the case under certain packing fractions and translational diffusive coefficients. And as we know Rouse theory<sup>34</sup> predicts significant subdiffusive behavior of the monomer mean square displacement (MSD) due to chain connectivity in the limit of long chains, with  $MSD \sim t^{0.5}$ . The work by Li et al<sup>35</sup> found activity in the unentangled semidilute polymer raises the ambient temperature, which significantly decreases diffusion by over an order of magnitude. But in this paper, activity is manifested as active reorientation capability, rather than activity enhanced by increasing temperature.

In the y direction (Fig. 8(c) and (d)), the situation is reversed. In the long time scale, the active system exhibits superdiffusive behavior under the same asymmetry, with higher diffusion intensity compared to the passive system. This is a particularly interesting finding. The reason is that mobility-induced phase separation which results from active parti-



cles with repulsive force causes the coupling between self-propelling and potential. According to previous results<sup>36,37</sup>, steady states of active systems with self-propulsion ability do not exhibit flocking behavior but mobility-induced phase separation. However, our system due to active reorientation displays collective flocking motion in the steady state when values of  $\alpha$  and  $D_r$  are relatively small<sup>29</sup>. Furthermore, during this steady state, the system no longer shows clustering<sup>29</sup>. Now, when an asymmetric potential trap is introduced, it significantly confines the active particles to one side. These active particles must interact closely while being confined together, continuously reorienting themselves. This, in turn, enhances the probability of particle overlap and reorienting, leading to a relatively quicker attainment of the flocking state or in other words, quickly reaching a stable state (see Fig. 3(a)). Finally under the same parameter  $c$ , there seems to be no significant difference in the x-direction between systems with active reorientation and those without active reorientation. However, in the y-direction, the system with active reorientation exhibits much stronger superdiffusive behavior compared to the system without active reorientation. The difference in MSD in the y direction also suggests that the potential in this direction is more complex or restrictive, making active reorientation a key factor in enhancing particle mobility.

## VI. CONCLUSION AND DISCUSSION

We explore the phase behaviors and dynamics of active systems with AR in a double-well potential. We obtain the phase diagram as a function of the asymmetry parameter of the potential and active reorientation. By comparing systems with and without AR, we find that the system with AR is sensitive to the asymmetry parameter of the potential. We also notice that the presence of active reorientation leads to a more pronounced caging effect. Finally, by calculating the mean squared displacement of the system, we reveal its diffusion regimes. Our results demonstrate the effect of potential on the dynamic behavior of various physical nonequilibrium systems with active reorientation.

## AUTHOR CONTRIBUTIONS

Lu Chen and Ning Liu conceived the project, and Lu Chen performed the research work, Ning Liu and Baopi Liu provided ideas and opinions. All authors wrote the paper jointly.

## CONFLICTS OF INTEREST

There are no conflicts to declare.

## ACKNOWLEDGEMENTS

We wish to acknowledge Z. C. Tu offering suggestions. We also acknowledge computational support from the Beijing Computational Science Research Center. The research was supported by the National Natural Science Foundation of China (Grant No. 11975050).

## DATA AVAILABILITY STATEMENT

The data that support the findings of this study is available from the corresponding author upon reasonable request.

- <sup>1</sup>M. E. Cates and J. Tailleur, *Annu. Rev. Condens. Matter Phys.* **6** (2015) 219.
- <sup>2</sup>P. de Castro, F. M. Rocha, S. Diles, R. Soto, and P. Sollich, *Soft Matter* **17** (2021) 9926.
- <sup>3</sup>F. Ginot, I. Theurkauff, F. Detcheverry, C. Ybert, and C. Cottin-Bizonne, in *Nature communications* **9** (2018) 696.
- <sup>4</sup>A. Cavagna, L. Del Castello, I. Giardina, T. Grigera, A. Jelic, S. Melillo, T. Mora, L. Parisi, E. Silvestri, M. Viale, et al., *J. STAT. PHYS* **158** (2015) 601.
- <sup>5</sup>T. Bertrand and C. F. Lee, *Phys. Rev. Res* **4** (2022) L022046.
- <sup>6</sup>A. Chardac, L. A. Hoffmann, Y. Poupard, L. Giomi, and D. Bartolo, *Phys. Rev. X* **11** (2021) 031069.
- <sup>7</sup>A. Morin, J. B. Caussin, C. Eloy, and D. Bartolo, *Phys. Rev. E* **91** (2015) 012134.
- <sup>8</sup>M. Casiulis and D. Levine, *Phys. Rev. E* **106** (2022) 044611.
- <sup>9</sup>D. Levis, I. Pagonabarraga, and B. Liebche, *Phys. Rev. Res* **1** (2019) 023026.
- <sup>10</sup>A. Morin and D. Bartolo, *Phys. Rev. X* **8** (2018) 021037.
- <sup>11</sup>L. Caprini, U. M. Bettolo Marconi, R. Wittmann, and H. Löwen, *SciPost Physics* **13** (2022) 065.
- <sup>12</sup>S. C. Takatori and J. F. Brady, *Soft Matter* **10** (2014) 9433.
- <sup>13</sup>R. Benjamin et al., *arXiv:2211.04298* (2022).
- <sup>14</sup>Y. Wu, A. Fu, and G. Yossifon, *Sci. Adv.* **1** (2020) eaay4412.
- <sup>15</sup>R. C. Maloney and C. K. Hall, *Langmuir* **36** (2020) 6378.
- <sup>16</sup>J. Bickmann, S. Bröker, and R. Wittkowski, *arXiv:2202.04423* (2022).
- <sup>17</sup>M. Kaiser, P. A. Sá nchez, N. Samanta, R. Chakrabarti, and S. S. Kantorovich, *The Journal of Physical Chemistry* **124** (2020) 8188.
- <sup>18</sup>A. Zakharchenko, N. Guz, A. M. Laradji, E. Katz, and S. Minko, *Nature Catalysis* **1** (2018) 73.
- <sup>19</sup>I. Abdoli and A. Sharma, *Soft Matter* **17** (2021) 1307.
- <sup>20</sup>W. ebeling, L. schimansky-geier, A. neiman, and A. scharnhorst, *Fluctuation and Noise Letters* **5** (2005) L185.
- <sup>21</sup>I. G. Marchenko, I. I. Marchenko, and A. Zhiglo, *Eur. Phys. J. B* **87** (2014) 1-7.
- <sup>22</sup>P. Zhou, X. Gao, X. Li, et al., *Phys. Rev. X* **11** (2021) 011004.
- <sup>23</sup>A. Militaru, M. Innerbichler, M. Frimmer, F. Tebbenjohanns, L. Novotny and C. Dellago *Nat. Commun.* **12** (2021) 2446.
- <sup>24</sup>L. Caprini, F. Cecconi and UMB. Marconi *J. Chem. Phys.* **155** (2021) 23.
- <sup>25</sup>Z. Li, Q. Cai, X. Zhang, et al., *Phys. Rev. Lett.* **118** (2017) 098101.
- <sup>26</sup>L. Chen, K. J. Welch, P. Leishangthem, D. Ghosh, B. Zhang, T. P. Sun, J. Klukas, Z. Tu, X. Cheng, and X. Xu, *arXiv:2302.10525* **36** (2023).
- <sup>27</sup>C. W. Reynolds, in *Proceedings of the 14th annual conference on Computer graphics and interactive techniques* (1987) pp. 25-34.
- <sup>28</sup>N. Kasmuri, N. Nazar, and A. Mohd Yazid, *Environment-Behaviour Proceedings Journal* **5** (2020) 315.
- <sup>29</sup>L. Chen, B. Zhang, and Z. Tu, *Chin. Phys. B* **32** (2023) 086401.
- <sup>30</sup>D. R. Rodriguez, F. Alarcon, R. Martinez, J. Ramirez, and C. Valeriani, *Soft Matter* **16** (2020) 1162.
- <sup>31</sup>J. Reichert, L. F. Granz, T. Voigtmann, *Eur. Phys. J. E* **44** (2021) 1-13.
- <sup>32</sup>A. Sharma, J. M. Brader, *J. Chem. Phys.* **145** (2016) 145.
- <sup>33</sup>J. Reichert, L. F. Granz, T. Voigtmann, *The European Physical Journal E* **44** (2021) 1-13.
- <sup>34</sup>M. Doi and S. F. Edwards, *Oxford University Press*, **20(26)** (1986) 5174-5182.

<sup>35</sup>J. Li, B. Zhang, and Z Y. Wang, *Soft Matter* **20(26)** (2024) 5174-5182.

<sup>36</sup>Y. Fily and M. C. Marchetti, *Phys. Rev. Lett.* **108** (2012) 235702.

<sup>37</sup>G. S. Redner, M. F. Hagan, and A. Baskaran, *Phys. Rev. Lett.* **36** (2013) 055701.